Published in final edited form as:
Biochem Biophys Res Commun. 2014 January 31; 444(1): 44–49. doi:10.1016/j.bbrc.2014.01.009.

KB-R7943, a plasma membrane Na^+/Ca^{2+} exchanger inhibitor, blocks opening of the mitochondrial permeability transition pore

Brian M. Wiczer, **Raluca Marcu**, and **Brian J. Hawkins***
Department of Anesthesiology and Pain Medicine, Mitochondria and Metabolism Center, University of Washington, Seattle, WA

Abstract

The isothiourea derivative, KB-R7943, inhibits the reverse-mode of the plasma membrane sodium/calcium exchanger and protects against ischemia/reperfusion injury. The mechanism through which KB-R7943 confers protection, however, remains controversial. Recently, KB-R7943 has been shown to inhibit mitochondrial calcium uptake and matrix overload, which may contribute to its protective effects. While using KB-R7943 for this purpose, we find here no evidence that KB-R7943 directly blocks mitochondrial calcium uptake. Rather, we find that KB-R7943 inhibits opening of the mitochondrial permeability transition pore in permeabilized cells and isolated liver mitochondria. Furthermore, we find that this observation correlates with protection against calcium ionophore-induced mitochondrial membrane potential depolarization and cell death, without detrimental effects to basal mitochondrial membrane potential or complex I-dependent mitochondrial respiration. Our data reveal another mechanism through which KB-R7943 may protect against calcium-induced injury, as well as a novel means to inhibit the mitochondrial permeability transition pore.

Keywords

calcium retention capacity; KB-R7943; permeability transition; mitochondria

1. Introduction

Mitochondrial Ca^{2+}-overload is a major contributor to ischemia/reperfusion injury [1–3]. Mechanistically, much of the organ damage associated with ischemia/reperfusion occurs during reperfusion as a result of a sudden elevation of cytosolic Ca^{2+} ($[Ca^{2+}]_c$). Mitochondria can rapidly sequester Ca^{2+} and act as an efficient buffering system to preserve cellular function [3]. However, the capacity of mitochondria to sequester Ca^{2+} is limited, and continued accumulation within the matrix will eventually impair mitochondrial function and bioenergetics. When this mitochondrial $[Ca^{2+}]$ ($[Ca^{2+}]_m$) threshold is reached, cyclophilin D activates the mitochondrial permeability transition pore (mPTP) to rapidly release matrix Ca^{2+} back into the cytosol [4]. mPTP activation subsequently triggers a loss of mitochondrial function and initiates cell death [3]. Indeed, pharmacologic or genetic

*Corresponding author: University of Washington, 850 Republican St, Room N-134, Seattle, WA, 98109-8057. Phone: 1-206-543-6140. bhawkins@uw.edu.

inactivation of the mPTP preserves mitochondrial function and organ health following ischemia/reperfusion [5]. However, pharmacologic mPTP blockers (i.e. cyclosporine A) have non-mitochondrial targets and are not practical therapeutic options. Agents that can inhibit the mPTP independent of cyclophilin D may serve as alternative therapies to reduce ischemia/reperfusion injury.

A primary cause of the elevated $[Ca^{2+}]_c$ observed during reperfusion is Ca^{2+} entry from the extracellular milieu via the reverse-mode of the plasma membrane Na^+/Ca^{2+} exchanger (NCX_{rev}) [6]. The isothiourea derivative, KB-R7943, is the prototypical inhibitor of NCX_{rev} [6,7]. Over the past decade, KB-R7943 has been used extensively to explore the effects of NCX_{rev} inhibition on ischemia/reperfusion injury, providing evidence that blocking NCX_{rev} is protective against ischemia/reperfusion-related myocardial [8–13] and neuronal damage [14–16]. Despite its apparent benefits, the precise mechanism through which KB-R7943 elicits protection remains controversial. In addition to the NCX_{rev}, KB-R7943 also lowers $[Ca^{2+}]_c$ by inactivating TRP channels [17], L-type voltage-gated Ca^{2+} channels [18], ryanodine receptors [19], NMDA receptors [20], and store-operated Ca^{2+} entry (SOCE) [21,22], though the specific molecular target of the latter is unknown. Despite these pharmacologic limitations and the availability of newer, more selective NCX_{rev} inhibitors [7], KB-R7943 is still widely used as an experimental tool to study ischemia/reperfusion injury. Recently, KB-R7943 was found to also potently reduce mitochondrial Ca^{2+} uptake by inhibiting the mitochondrial Ca^{2+} uniporter (MCU) [23], which would effectively reduce mPTP activation during reperfusion. However, the original finding that KB-R7943 acts as an MCU inhibitor is not entirely consistent with results in subsequent studies [14,20] and requires further evaluation.

During our studies aimed at perturbing mPTP activation and mitochondrial Ca^{2+} uptake, we utilized KB-R7943 in AD293 cells that do not express any of the NCX isoforms [24,25] and lack other known targets. Surprisingly, we discovered that KB-R7943 does not block mitochondrial Ca^{2+} uptake. Rather, KB-R7943 influences mitochondrial Ca^{2+} handling by increasing the Ca^{2+} retention capacity (CRC), which we demonstrate protects mitochondrial function from pathological Ca^{2+} overload. As such, KB-R7943 may serve as a novel mPTP inhibitor in certain contexts as an alternative to cyclosporine A and its analogues.

2. Materials and Methods

2.1. Cell culture and reagents

KB-R7943 (2-[2-[4-(4-nitrobenzyloxy)phenyl]ethyl]isothiourea) mesylate and CGP-37157 (7-Chloro-5-(2-chlorophenyl)-1,5-dihydro-4,1-benzothiazepin-2(3*H*)-one) were purchased from Tocris. Fura-2/AM, Fura-FF pentapotassium salt, tetramethylrhodamine ethyl ester (TMRE), JC-1, propidium iodide, Hoechst 33342, pluronic F-127, as well as all cell culture reagents including 50× MEM amino acids, 100× MEM non-essential amino acids (NEAA), 100× sodium pyruvate and 200mM Lglutamine were purchased from Life Technologies. Cyclosporine A (CsA), ruthenium red (RR), ionomycin, and all other chemicals were obtained from Sigma. HeLa cells and AD293 cells (Stratagene) were maintained in high glucose DMEM (Life Technologies, #11995-065) supplemented with 10% fetal bovine serum (Life Technologies) in a humidified cell culture incubator.

2.2. Fluorescence microscopy and spectrofluorometry

Fluorescence images were acquired using a Nikon Eclipse Ti microscope equipped with a xenon arc lamp and DeltaRamX monochromator (Photon Technology International), captured with an Evolve 512 EMCCD (Photometrics) with the assistance of EasyRatioPro software. Fura-2 was excited at 340 nm and 380 nm and fluorescence detected using a 400

nm long-pass dichroic mirror and 510/80m emission filter. TMRE and propidium iodide (PI) were excited at 545 nm and 535 nm, respectively and fluorescence detected using a 565 nm long-pass dichroic mirror and 610/75m emission filter. Hoechst 33342 was excited at 360 nm and fluorescence detected as fura-2. A Nikon 40X Plan Fluor oil immersion lens objective was used to image fura-2 and TMRE. PI and Hoechst 33342 were imaged with a Nikon 10X Ph1 ADL objective.

Spectrofluorometric studies were performed as previously described [26].

2.3. Isolation of mouse liver mitochondria

Liver mitochondria were isolated from FVB/N mice aged 3–6 months using differential centrifugation as previously described [27]. Isolated mitochondria were then resuspended in a minimal amount of mitochondrial isolation buffer plus 0.1% BSA and kept on ice. All steps were performed on ice and using refrigerated centrifuges set to 4°C. Protein concentration was determined by Bradford method. Mitochondria were used within 4 hours.

2.4. Measurement of mitochondrial respiration

Mitochondrial respiration was assessed in permeabilized cells as described previously [28]. Briefly, AD293 cells were seeded at 1.5×10^6 cells per 10-cm culture dish. Two days later, cells were harvested in 1mL ambient temperature PBS using a cell lifter, briefly pelleted, and washed 1x with pre-warmed (30°C) respiration medium (20 mM HEPES, pH 7.1 at 30°C, 64 mM KCl, 3 mM $MgCl_2$, 0.5 mM EGTA, 110 mM mannitol, 10 mM KH_2PO_4, 0.3 mM DTT). Cells were pelleted and resuspended in respiration medium with 40 μg/mL digitonin and added to a calibrated Oxytherm chamber (Hansatech). Permeabilization was allowed to occur for 5 minutes, with subsequent addition of 5 mM sodium pyruvate/2.5 mM malate to initiate state 2 respiration. 2 mM Mg^{2+}-ADP was added to initiate state 3 respiration.

2.5. Live cell imaging of cytosolic Ca^{2+} ($[Ca^{2+}]_c$) and mitochondrial membrane potential ($\Delta\psi_m$)

Forty thousand AD293 cells were plated onto glass-bottom MatTek dishes coated with Cell-Tak (BD Biosciences), and media was replaced after one day with low serum (0.5% FBS) DMEM with 20 mM HEPES, pH 7.4. For imaging $[Ca^{2+}]_c$, cells were loaded with 5 μM fura-2/AM for 20 minutes at ambient temperature in a modified DMEM-like Krebs-Ringers-HEPES-bicarbonate (KRHB) buffer (20 mM HEPES, 120 mM NaCl, 4.8 mM KCl, 1.2 mM KH_2PO_4, 1.2 mM $MgSO_4$, 1.8 mM $CaCl_2$, 5 mM $NaHCO_3$, 25 mM glucose, 1 mM sodium pyruvate, 2 mM L-glutamine, 1x MEM AA, 1x MEM NEAA, pH 7.4), with 0.006% (w/v) pluronic F-127, and 100 μM sulfinpyrazone. Cells were subsequently washed with and imaged in KRHB plus 100 μM sulfinpyrazone. Images were acquired every 4 seconds and the nuclear 340 nm/380 nm fluorescence ratio was calculated and applied to a predetermined $[Ca^{2+}]_c$ calibration curve.

Cellular $\Delta\psi_m$ was evaluated using 50 nM TMRE in modified KRHB buffer. Cells were washed 1x with TMRE-free KRHB (pH 7.4) and imaged in KRHB at ambient temperature and atmosphere. Images were acquired every 60 seconds to obtain mitochondrial TMRE fluorescence. Individual traces were normalized to the initial fluorescence intensity.

2.6. Measurements of mitochondrial Ca^{2+} uptake and $\Delta\psi_m$ in permeabilized cells and isolated mitochondria

Mitochondrial Ca^{2+} uptake and $\Delta\psi_m$ were measured in permeabilized cells or isolated mitochondria as previously described [26]. Briefly, cells were seeded onto 6 cm culture plates and serum deprived as above. On the following day, the confluent monolayers were

washed in ice-cold extracellular medium (ECM) (20 mM HEPES, 120 mM Nalco, 5 mM KCl, 1 mM KH_2PO_4, 0.2 mM $MgCl_2$, 0.1 mM EGTA, pH 7.4 at 0°C), harvested in ECM using a cell lifter, and left on ice for 20 minutes. Cells were then washed in ice-cold PBS and immediately resuspended in 1 mL of pre-warmed (30°C) mitochondria assay buffer (MAB) plus 40 μg/mL digitonin and 1 μM thapsigargin ([DMSO] = 0.2% (v/v)), and inserted into the spectrofluorometer set to 30°C. Cells were allowed to permeabilize for 5 minutes in the presence of 5 mM sodium pyruvate/2.5 mM malate, and 1.25 μM Fura-FF or 500 nM JC-1 to measure Ca^{2+} uptake or $\Delta\psi_m$, respectively. Isolated liver mitochondria (0.25 mg/mL) were incubated in MAB, without digitonin and thapsigargin, in the presence of substrates and dyes for 5 minutes. Both permeabilized cells and isolated mitochondria were pulsed with 3 nmol $CaCl_2$.

2.7. Cell death analysis

AD293 cells were plated at 5×10^5 cells per well of a 6-well plate coated with 0.1% gelatin. Next day, cells were refreshed with media. 24 hours later, media was replaced with a modified DMEM-like KRHB buffer. Cells were treated with 1.5 μM ionomycin for 5 hours at 37°C in culture incubator. PI (1μg/mL) and Hoechst 33342 (5 μg/mL) were added 1 hour prior to fluorescence microscopic imaging. For each experiment, 6 fields were acquired per condition. Fluorescent nuclei were counted using ImageJ, and cell death calculated as the percentage PI positive nuclei relative to Hoechst 33342 nuclei.

2.8. Statistical analysis

Values are expressed as the mean ± standard error of the mean (SEM). Student's *t*-test, or one-way ANOVA or two-way ANOVA with a Dunnett's multiple comparisons test were performed where appropriate using GraphPad Prism v6.0. Differences were considered statistically significant if $p < 0.05$.

3. Results and Discussion

3.1. KB-R7943 does not inhibit mitochondrial Ca^{2+} uptake in permeabilized cells

Mitochondrial Ca^{2+} uptake was evaluated in permeabilized AD293 (Fig. 1A) and HeLa (Fig. 1B) cells as the depletion rate of extramitochondrial calcium using membrane-impermeant Fura-FF in response to 3 nmol Ca^{2+} pulses. In both AD293 and HeLa cells, Ca^{2+} was rapidly taken up by mitochondria and effectively blocked by the traditional MCU inhibitor, ruthenium red (RR) (Fig. 1). Individually, RR elicited a rapid increase in extramitochondrial Ca^{2+} which was ablated in the presence of the mitochondrial Na^+/Ca^{2+}-exchanger CGP-37157 (data not shown), implying there is a continuous flux of mitochondrial Ca^{2+} [29]. Surprisingly, mitochondrial Ca^{2+} uptake was not inhibited in the presence of KB-R7943 at either 10 or 20 μM, contrary to the previous initial report [23]. It is unclear why our results differ considering that HeLa cells were used in both cases. While different experimental techniques were used to measure mitochondrial Ca^{2+} uptake (i.e., increase in $[Ca^{2+}]_m$ using targeted aequorin in the former study versus decrease in extramitochondrial Ca^{2+} in the present work), both methods have been validated to measure changes in mitochondrial Ca^{2+} uptake [30]. However, evaluating the technical merits of aequorin versus Fura-FF was not a focus of our research and requires further testing. Nonetheless, our observations are consistent with previous reports that also imply Ca^{2+} uptake into isolated brain mitochondria is not blocked by KB-R7943 [14,20]. Together, these findings suggest that KB-R7943 does not directly influence mitochondrial Ca^{2+} uptake and that caution should be applied when using this compound to evaluate mitochondrial Ca^{2+} dynamics.

3.2. KB-R7943 increases the mitochondrial Ca^{2+} retention capacity

Despite no detectable effect on Ca^{2+} uptake, we unexpectedly noticed that KB-R7943 did consistently increase the number of Ca^{2+} pulses that could be effectively sequestered by permeabilized cells. Indeed, direct evaluation of this observation revealed that KB-R7943 addition resulted in a dose-dependent increase in the number of Ca^{2+} pulses required to engage the mPTP (Fig. 2A). The number of Ca^{2+} pulses required to open the mPTP was counted and quantified as the mitochondrial Ca^{2+} retention capacity (CRC) (Fig. 2B) [31]. A similar increase in CRC was also found in HeLa cells (Fig. 2C) and in isolated liver mitochondria (Fig. 2D), demonstrating that the effect of KB-R7943 on the CRC is a ubiquitous phenomenon. KB-7943 was not, however, as effective as the classical mPTP inhibitor, CsA, at increasing the CRC (Fig. 2A). However, KB-R7943 nearly doubled CsA-mediated mPTP inhibition (data not shown), hinting that these pharmacologic agents behave synergistically and have distinct molecular targets.

3.3. KB-R7943 protects against Ca^{2+}-induced mitochondrial depolarization and cell death

If indeed KB-R7943 increases the CRC, we hypothesized that it might also attenuate mPTP opening and mitochondrial membrane potential ($\Delta\psi_m$) loss in response to mitochondrial Ca^{2+} overload. We therefore utilized the Ca^{2+} ionophore, ionomycin, to activate the mPTP in a Ca^{2+}-dependent manner [32–36]. AD293 cells loaded with the cationic fluorophore TMRE were visualized using real-time fluorescence microscopy to assess relative changes in $\Delta\psi_m$ in response to 4 μM ionomycin. As predicted, ionomycin challenge evoked a time-dependent $\Delta\psi_m$ depolarization (Fig. 3A). In contrast, $\Delta\psi_m$ loss was prevented by 20 μM KB-R7943, consistent with the ability of KB-R7943 to increase the CRC.

Because KB-R7943 blocked Ca^{2+}-induced mPTP opening and $\Delta\psi_m$ depolarization, we posited that it would also protect against Ca^{2+}-induced cell death. To test this hypothesis, AD293 cells were treated with ionomycin for 5 hours and cell death quantified as the percentage of cells staining positive for the membrane impermeable propidium iodide (PI), which incorporates into the nucleus when the plasma membrane is compromised. Supportive of our hypothesis, we found that KB-R7943 attenuated ionomycin-induced cell death (Fig. 3B–C). In light of these findings, it is possible that some of the published benefits of KB-R7943 in ischemia/reperfusion injury may stem from an inhibition of the mPTP and mitochondrial-mediated cell death.

3.4. Effect of KB-R7943 on basal $\Delta\psi_m$ and mitochondrial respiration

Previous reports purport that KB-R7943 is neuroprotective effect due in part to mild $\Delta\psi_m$ depolarization and complex I inhibition [14,20]. Thus, it is possible that the effects of KB-R7943 against Ca^{2+}-induced $\Delta\psi_m$ depolarization in our system may be due to an adaptive response incurred by mild mitochondrial dysfunction in addition to increasing the CRC. Furthermore, complex I inhibition can alone increase the CRC in both permeabilized cells and isolated mitochondria [31], though this was demonstrated in the presence of the complex II substrate, succinate. Therefore, we assessed complex I-dependent basal $\Delta\psi_m$ and mitochondrial respiration in permeabilized AD293 cells in response to KB-R7943. Using the ratiometric $\Delta\psi_m$ indicator, JC-1, mitochondria energized with complex I substrates (pyruvate+malate) did not exhibit a reduction in $\Delta\psi_m$ following KB-R7943 addition. Rather, we observed a slight hyperpolarization in $\Delta\psi_m$ relative to vehicle treated cells (Fig. 4A). A single Ca^{2+} pulse did, however, produce a transient decrease in $\Delta\psi_m$ indicative of the transmembrane import of positively-charged Ca^{2+} into the matrix [37]. This slight reduction in $\Delta\psi_m$ was unaffected by KB-R7943, providing further support that KB-R7943 does not impact mitochondrial Ca^{2+} import (Fig. 1). Aside from $\Delta\psi_m$, KB-R7943 did not affect mitochondrial state 2 or state 3 respiration at any of the doses tested (Fig. 4B). Taken together, these data demonstrate that the protective effect of KB-R7943 on Ca^{2+}-induced

mPTP opening and cell death is not due to mitochondrial respiratory impairment and $\Delta\psi_m$ alterations, but rather, to its ability to increase mitochondrial Ca^{2+} handling capacity.

As we find no negative impact of KB-R7943 on $\Delta\psi_m$ and respiration, it is unclear why our results contrast those found in similar experiments performed using brain mitochondria [20]. In those studies, KB-R7943 decreased the CRC of brain mitochondria when energized on complex I substrates [20] and runs counter to our present results. It should be noted that the decrease in CRC they observed was due to a respiration-dependent inhibition of mitochondrial Ca^{2+} uptake after reaching some $[Ca^{2+}]_m$-threshold rather than due to an effect on mPTP opening. Therefore, this apparent discrepancy may highlight a phenotypic difference between neuronal and non-neuronal mitochondria. While we demonstrate that KB-R7943 inhibits Ca^{2+}-dependent mPTP opening in multiple systems, the exact mechanism remains elusive. Nonetheless, while KB-R7943 is clearly a promiscuous pharmacologic agent with multiple Ca^{2+}-regulatory targets, it may serve as a novel mPTP inhibitor in certain contexts as an alternative to cyclosporine A and its analogues.

Acknowledgments

We would like to thank Stephen Kolwicz and Rong Tian for experimental assistance. This research was supported by HL094536 and a UW RRF award to B.J.H.

References

1. Crompton M. The mitochondrial permeability transition pore and its role in cell death. Biochem. J. 1999; 341(Pt 2):233–249. [PubMed: 10393078]
2. Hansson MJ, Persson T, Friberg H, Keep MF, Rees A, Wieloch T, et al. Powerful cyclosporin inhibition of calcium-induced permeability transition in brain mitochondria. Brain Res. 2003; 960:99–111. [PubMed: 12505662]
3. Duchen MR. Roles of mitochondria in health and disease. Diabetes. 2004; 53(Suppl 1):S96–S102. [PubMed: 14749273]
4. Petronilli V, Miotto G, Canton M, Brini M, Colonna R, Bernardi P, et al. Transient and Long-Lasting Openings of the Mitochondrial Permeability Transition Pore Can Be Monitored Directly in Intact Cells by Changes in Mitochondrial Calcein Fluorescence. Biophysical Journal. 1999; 76:725–734. [PubMed: 9929477]
5. Baines CP, Kaiser RA, Purcell NH, Blair NS, Osinska H, Hambleton MA, et al. Loss of cyclophilin D reveals a critical role for mitochondrial permeability transition in cell death. Nature. 2005; 434:658–662. [PubMed: 15800627]
6. Watano T. A Novel Isothiourea Derivative Selectively Inhibits the Reverse Mode of Na+/Ca2+ Exchange in Cells Expressing NCX1. Journal of Biological Chemistry. 1996; 271:22391–22397. [PubMed: 8798401]
7. Iwamoto T, Watanabe Y, Kita S, Blaustein MP. Na+/Ca2+ exchange inhibitors: a new class of calcium regulators. Cardiovasc Hematol Disord Drug Targets. 2007; 7:188–198. [PubMed: 17896959]
8. Motegi K, Tanonaka K, Takenaga Y, Takagi N, Takeo S. Preservation of mitochondrial function may contribute to cardioprotective effects of Na+/Ca2+ exchanger inhibitors in ischaemic/reperfused rat hearts. British Journal of Pharmacology. 2007; 151:963–978. [PubMed: 17549042]
9. Magee WP, Deshmukh G, Deninno MP, Sutt JC, Chapman JG, Tracey WR. Differing cardioprotective efficacy of the Na+/Ca2+ exchanger inhibitors SEA0400 and KB-R7943. Am. J. Physiol. Heart Circ. Physiol. 2003; 284:H903–H910. [PubMed: 12446284]
10. Hagihara H, Yoshikawa Y, Ohga Y, Takenaka C, Murata K-Y, Taniguchi S, et al. Na+/Ca2+ exchange inhibition protects the rat heart from ischemiareperfusion injury by blocking energy-wasting processes. Am. J. Physiol. Heart Circ. Physiol. 2005; 288:H1699–707. [PubMed: 15626686]

11. Inserte J, Garcia-Dorado D, Ruiz-Meana M, Padilla F, Barrabés JA, Pina P, et al. Effect of inhibition of Na(+)/Ca(2+) exchanger at the time of myocardial reperfusion on hypercontracture and cell death. Cardiovascular Research. 2002; 55:739–748. [PubMed: 12176123]
12. Takahashi K, Takahashi T, Suzuki T, Onishi M, Tanaka Y, Hamano- Takahashi A, et al. Protective effects of SEA0400, a novel and selective inhibitor of the Na+/Ca2+ exchanger, on myocardial ischemia-reperfusion injuries. European Journal of Pharmacology. 2003; 458:155–162. [PubMed: 12498920]
13. Yoshitomi O, Akiyama D, Hara T, Cho S, Tomiyasu S, Sumikawa K. Cardioprotective effects of KB-R7943, a novel inhibitor of Na+/Ca2+ exchanger, on stunned myocardium in anesthetized dogs. J Anesth. 2005; 19:124–130. [PubMed: 15875129]
14. Storozhevykh TP, Senilova YE, Brustovetsky T, Pinelis VG, Brustovetsky N. Neuroprotective Effect of KB-R7943 Against Glutamate Excitotoxicity is Related to Mild Mitochondrial Depolarization. Neurochem Res. 2009; 35:323–335. [PubMed: 19771515]
15. Hoyt KR, Arden SR, Aizenman E, Reynolds IJ. Reverse Na+/Ca2+ exchange contributes to glutamate-induced intracellular Ca2+ concentration increases in cultured rat forebrain neurons. Molecular Pharmacology. 1998; 53:742–749. [PubMed: 9547366]
16. Martínez-Sánchez M, Striggow F, Schröder UH, Kahlert S, Reymann KG, Reiser G. Na(+) and Ca(2+) homeostasis pathways, cell death and protection after oxygen-glucose-deprivation in organotypic hippocampal slice cultures. Neuroscience. 2004; 128:729–740. [PubMed: 15464281]
17. Kraft R. The Na+/Ca2+ exchange inhibitor KB-R7943 potently blocks TRPC channels. Biochemical and Biophysical Research Communications. 2007; 361:230–236. [PubMed: 17658472]
18. Ouardouz M, Zamponi GW, Barr W, Kiedrowski L, Stys PK. Protection of ischemic rat spinal cord white matter: Dual action of KB-R7943 on Na+/Ca2+ exchange and L-type Ca2+ channels. Neuropharmacology. 2005; 48:566–575. [PubMed: 15755484]
19. Barrientos G, Bose DD, Feng W, Padilla I, Pessah IN. The Na+/Ca2+ exchange inhibitor 2-(2-(4-(4-nitrobenzyloxy)phenyl)ethyl)isothiourea methanesulfonate (KB-R7943) also blocks ryanodine receptors type 1 (RyR1) and type 2 (RyR2) channels. Molecular Pharmacology. 2009; 76:560–568. [PubMed: 19509218]
20. Brustovetsky T, Brittain MK, Sheets PL, Cummins TR, Pinelis V, Brustovetsky N. KB-R7943, an inhibitor of the reverse Na+/Ca2+ exchanger, blocks N-methyl-D-aspartate receptor and inhibits mitochondrial complex I. British Journal of Pharmacology. 2010; 162:255–270. [PubMed: 20883473]
21. Arakawa N, Sakaue M, Yokoyama I, Hashimoto H, Koyama Y, Baba A, et al. KB-R7943 Inhibits Store-Operated Ca2+ Entry in Cultured Neurons and Astrocytes. Biochemical and Biophysical Research Communications. 2000; 279:354–357. [PubMed: 11118291]
22. Birnbaumer, L.; Yildirim, E.; Liao, Y. Molecular and functional diversity of the TRPC family of ion channels. TRPC channels and their role in ROCE/SOCE. In: Conn, M.; Christen, Y.; Kordon, C., editors. Insights into Receptor Function and New Drug Development Targets. Springer; 2006. p. 1-22.
23. Santo-Domingo J, Vay L, Hernández-SanMiguel E, Lobatón CD, Moreno A, Montero M, et al. The plasma membrane Na +/Ca 2+exchange inhibitor KBR7943 is also a potent inhibitor of the mitochondrial Ca 2+uniporter. British Journal of Pharmacology. 2007; 151:647–654. [PubMed: 17471180]
24. Hurtado C, Prociuk M, Maddaford TG, Dibrov E, Mesaeli N, Hryshko LV, et al. Cells expressing unique Na+/Ca2+ exchange (NCX1) splice variants exhibit different susceptibilities to Ca2+ overload. Am. J. Physiol. Heart Circ. Physiol. 2006; 290:H2155–62. [PubMed: 16399865]
25. Rahamimoff H, Elbaz B, Alperovich A, Kimchi-Sarfaty C, Gottesman MM, Lichtenstein Y, et al. Cyclosporin A-dependent downregulation of the Na+/Ca2+ exchanger expression. Ann. N. Y. Acad. Sci. 2007; 1099:204–214. [PubMed: 17446460]
26. Marcu R, Neeley CK, Karamanlidis G, Hawkins BJ. Multi-parameter measurement of the permeability transition pore opening in isolated mouse heart mitochondria. J Vis Exp. 2012

27. Marcu R, Rapino S, Trinei M, Valenti G, Marcaccio M, Pelicci PG, et al. Electrochemical study of hydrogen peroxide formation in isolated mitochondria. Bioelectrochemistry. 2012; 85:21–28. [PubMed: 22197548]
28. Kuznetsov AV, Veksler V, Gellerich FN, Saks V, Margreiter R, Kunz WS. Analysis of mitochondrial function in situ in permeabilized muscle fibers, tissues and cells. Nat Protoc. 2008; 3:965–976. [PubMed: 18536644]
29. Malli R, Frieden M, Osibow K, Zoratti C, Mayer M, Demaurex N, et al. Sustained Ca2+ transfer across mitochondria is Essential for mitochondrial Ca2+ buffering, sore-operated Ca2+ entry, and Ca2+ store refilling. JBiol. Chem. 2003; 278:44769–44779. [PubMed: 12941956]
30. Pan X, Liu J, Nguyen T, Liu C, Sun J, Teng Y, et al. Nat Cell Biol 2013 Pan X. Nature Cell Biology. 2013; 5:1–12.
31. Li B, Chauvin C, De Paulis D, De Oliveira F, Gharib A, Vial G, et al. Inhibition of complex I regulates the mitochondrial permeability transition through a phosphate-sensitive inhibitory site masked by cyclophilin D. BBA - Bioenergetics. 2012; 1817:1628–1634. [PubMed: 22659400]
32. Abramov AY, Duchen MR. Actions of ionomycin, 4-BrA23187 and a novel electrogenic Ca2+ ionophore on mitochondria in intact cells. Cell Calcium. 2003; 33:101–112. [PubMed: 12531186]
33. Huang W-Y, Jou M-J, Peng T-I. Hypoxic preconditioning-induced mitochondrial protection is not disrupted in a cell model of mtDNA T8993G mutation-induced F1F0-ATP synthase defect: the role of mitochondrial permeability transition. Free Radical Biology and Medicine. 2013
34. Tazawa H, Fujita C, Machida K, Osada H, Ohta Y. Involvement of cyclophilin D in mitochondrial permeability transition induction in intact cells. Archives of Biochemistry and Biophysics. 2009; 481:59–64. [PubMed: 18996353]
35. Tornero D, Posadas I, Ceña V. Bcl-x(L) blocks a mitochondrial inner membrane channel and prevents Ca2+ overload-mediated cell death. PLoS ONE. 2011; 6:e20423. [PubMed: 21674052]
36. Choo H-J, Saafir TB, Mkumba L, Wagner MB, Jobe SM. Mitochondrial calcium and reactive oxygen species regulate agonist-initiated platelet phosphatidylserine exposure. Arteriosclerosis, Thrombosis, and Vascular Biology. 2012; 32:2946–2955.
37. Mitchell P. Chemiosmotic coupling in oxidative and photosynthetic phosphorylation. Biol Rev Camb Philos Soc. 1966; 41:445–502. [PubMed: 5329743]

Abbreviations

NCX_{rev}	reverse-mode of NCX
mPTP	mitochondrial permeability transition pore
CRC	mitochondrial calcium retention capacity
$\Delta\psi_m$	mitochondrial membrane potential
ECM	extracellular medium
MAB	mitochondria assay buffer
KRHB	Krebs-Ringers-HEPES-bicarbonate

Highlights

- KB-R7943 did not block mitochondrial calcium uptake.
- KB-R7943 increased the mitochondrial calcium retention capacity.
- KB-R7943 protected against Ca^{2+} ionophore-induced mPTP opening and cell death.

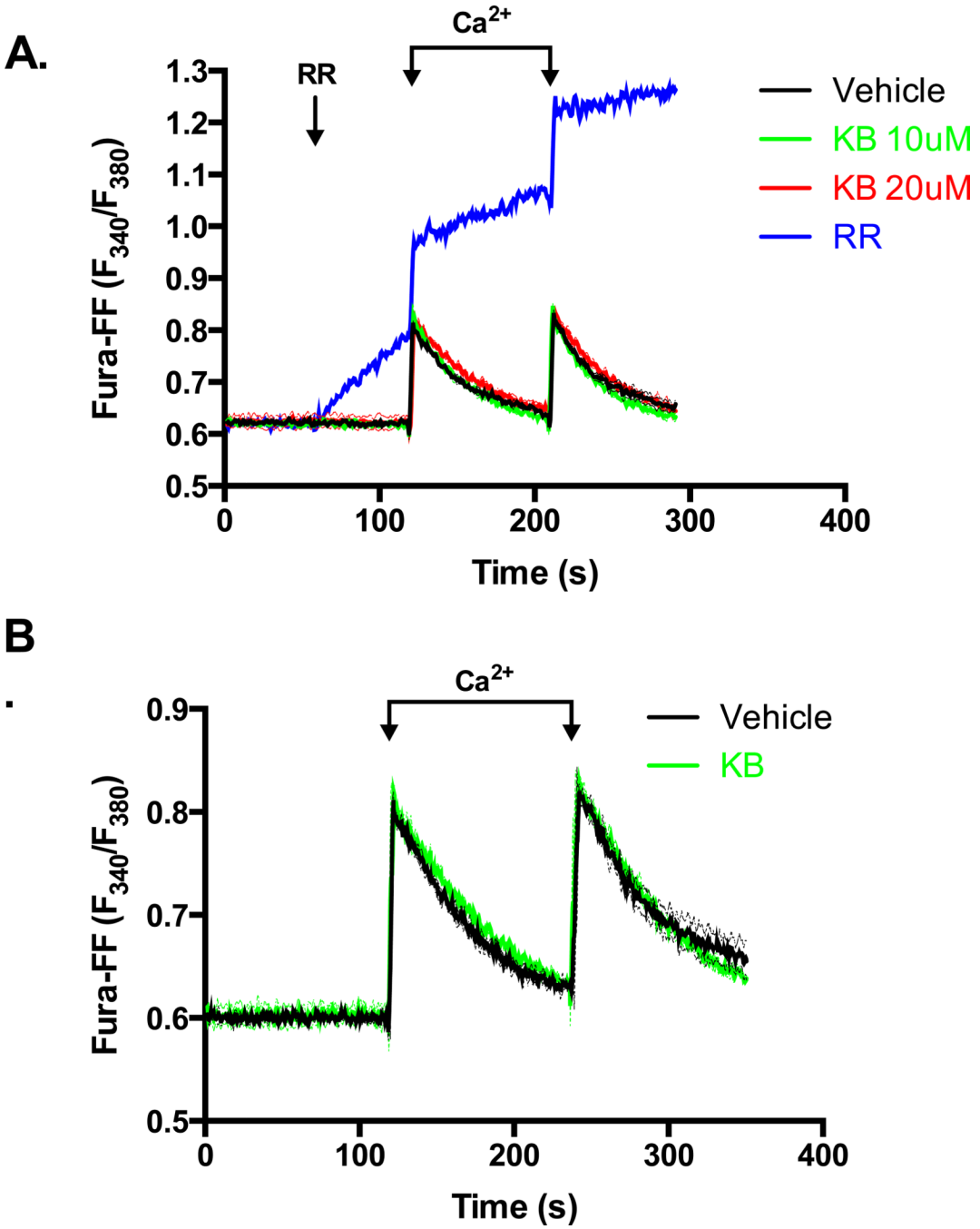

Fig. 1.

KB-R7943 does not inhibit mitochondrial Ca^{2+} uptake. Permeabilized AD293 cells (A) and HeLa cells (B) were pulsed with 3 nmol Ca^{2+} where indicated. The indicated concentration of KB-R7943 (20 μM in (B)) was added at the onset of permeabilization and present throughout the experiment. Vehicle is 0.05% DMSO, making the total [DMSO] per experiment 0.25% (v/v). In (A), ruthenium red (RR, 2 μM) was added where indicated. Traces are represented as the mean (solid lines) ± SEM (dashed lines) of 3 independent experiments. The RR positive control is a single trace from a representative experiment.

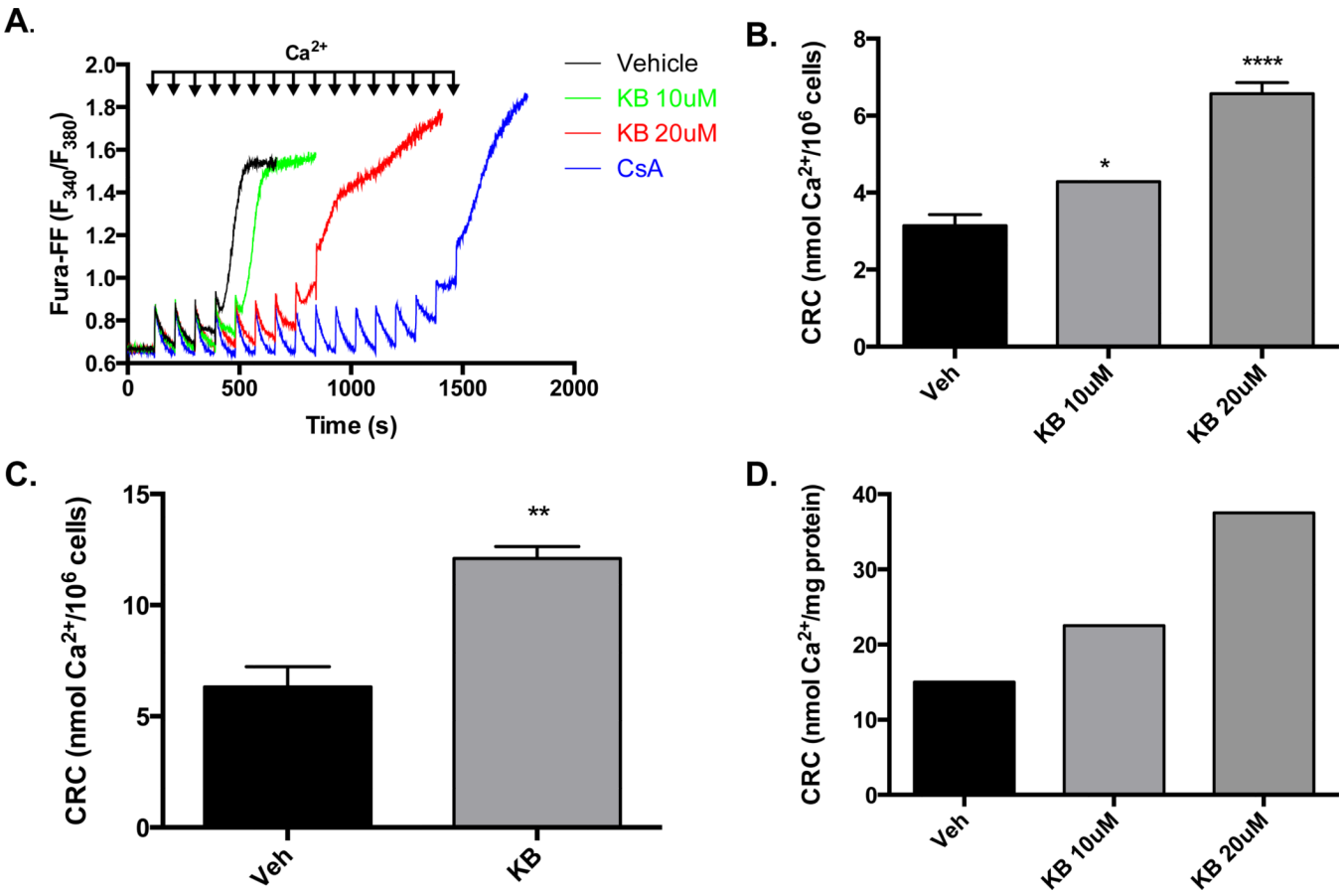

Fig. 2.

KB-R7943 increases mitochondrial Ca^{2+} retention capacity. Ca^{2+} pulses were administered as in Fig. 1 to activate the mPTP. KB-R7943 or CsA (1 μM) was added five minutes prior to the start of data acquisition. (A) Data are representative traces obtained during experiments using permeabilized AD293 cells. (B–D) Graphical representation of Ca^{2+} retention capacity (CRC) as calculated from data obtained in experiments similar to (A). CRC was determined in permeabilized AD293 cells (B) and HeLa cells (C), and isolated liver mitochondria (D). CRC = (number of Ca^{2+} pulses required to open the PTP) × (nmol Ca^{2+}/pulse). (B and C) Data represented as the mean ± SEM of 3 independent experiments. *, $p < 0.05$; **, $p < 0.01$; ****, $p < 0.0001$ as compared to vehicle. (D) Data represented as the mean ± SEM of 3 experiments from one mouse liver preparation.

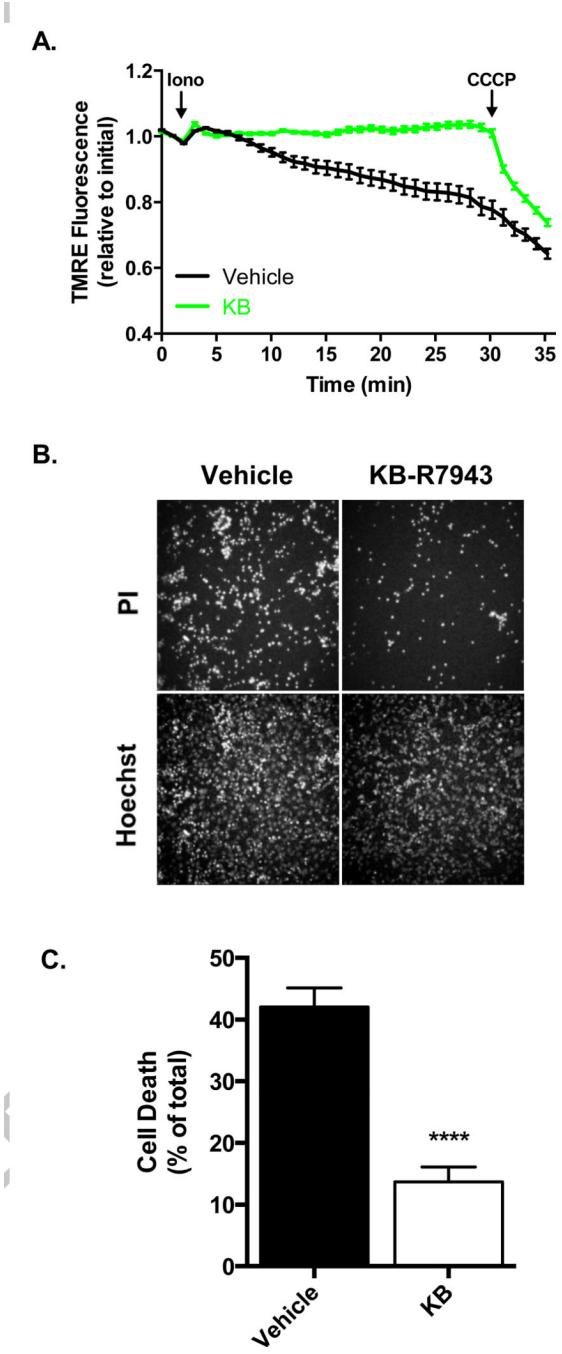

Fig. 3.

KB-R7943 protects against ionomycin-induced $\Delta\psi_m$ depolarization and cell death. (A) AD293 cells were loaded with TMRE in the presence of vehicle (0.2% DMSO) or 20 μM KB-R7943. Cells were subsequently treated with 4 μM ionomycin and single-cell fluorescence measurements were taken every minute. At the end of every experiment, 1 μM CCCP was added to depolarize $\Delta\psi_m$ in all cells. The data are represented as the mean ± SEM of n = 124 cells and n = 128 cells for vehicle- and KB-R7943-treated cells, respectively, obtained from 3 independent experiments. (B–C) AD293 cells were pretreated with vehicle or 20 μM KB-R7943 for 10 minutes prior to the addition of 1.5 μM ionomycin. Propidium iodide (PI) and Hoechst 33342 fluorescence was assessed after 5 hours. (B)

Representative images of stained cells post-treatment. (C) Graphical representation of images acquired. Cell death percentage for each field was quantified as the (# of PI-positive cells / # of Hoechst-positive cells) × 100%. The data are represented as the mean ± SEM of n = 6 fields and representative of 3 independent experiments. ****, $p < 0.0001$ relative to vehicle.

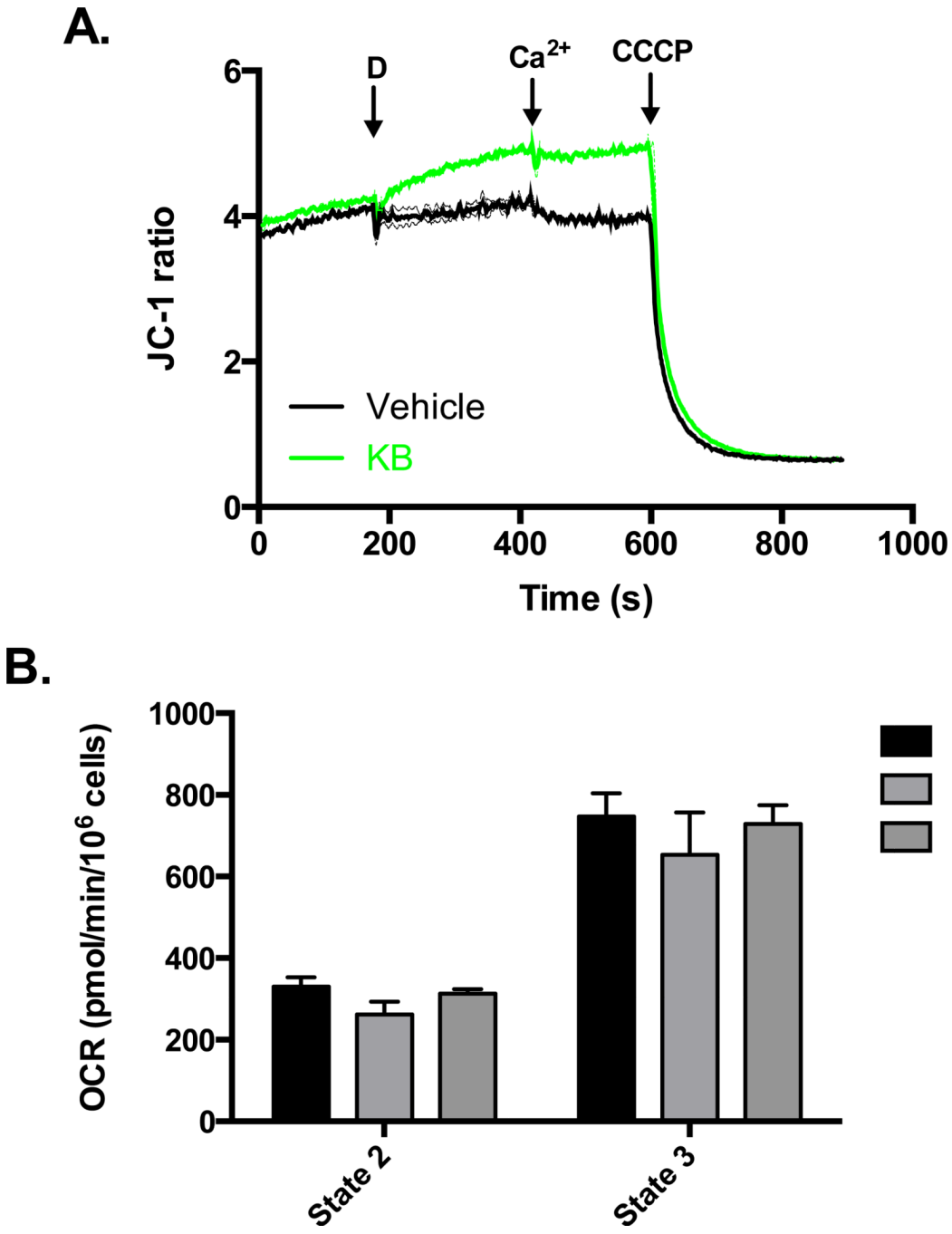

Fig. 4.

KB-R7943 increases $\Delta\psi_m$ but does not effect mitochondrial respiration. (A) Permeabilized AD293 cells were incubated with JC-1 during permeabilization to allow aggregate/monomer equilibration. After baseline JC-1 ratio (aggregate/monomer fluorescence) was acquired, 20 μM KB-R7943 or vehicle (0.05% DMSO) was added where indicated (***D***). After stabilization of JC-1 ratio, 3 nmol Ca^{2+} was added where indicated (***Ca*$^{2+}$**), followed by addition of 1 μM CCCP to achieve complete $\Delta\psi_m$ depolarization. Data are represented as the mean (solid line) ± SEM (dashed line) of 2 independent experiments. (B) Mitochondrial respiration of permeabilized AD293 was measured using 5 mM pyruvate/2.5 mM malate

with (**state 3**) or without (**state 2**) ADP. 10 or 20 μM KB-R7943 was added during permeabilization. O_2 consumption was measured during state 2 for at least two minutes before initiating state 3. O_2 consumption rate (OCR) was calculated from the slopes of the acquired traces. Data represented as the mean ± SEM of 3 experiments.